Korean J. Chem. Eng., **22**(5), 774-782 (2005)

Performance Evaluation of a Pilot Scale Vortexing Fluidized Bed Combustor

Chien-Song Chyang†, Kuo-Chao Lo and Kuo-Lian Wang

Department of Chemical Engineering, Chung Yuan Christian University, Chung-Li 320, Taiwan, R.O.C.
(*Received 4 February 2005 • accepted 7 June 2005*)

Abstract−To understand vortexing fluidized bed combustor (VFBC) performances, an investigation was carried out in a 0.45 m diameter and 4.45 m height pilot scale VFBC. Rice husks, corn, and soybean were used as the biomass feedstock and silica sand serving as the bed material. The bubbling bed temperature was controlled by using water injected into the bed. The experimental results show that the excess air ratio is the dominant factor for combustion efficiency. The in-bed combustion proportion increases with the primary air flow rate and bed temperature, and decreases with the volatile/fixed carbon ratio. The stability constant is proposed to describe the inertia characteristics of the vortexing fluidized bed combustor. The experimental results indicate that the stability of the VFBC increases with bed weight and primary air flow rate, but decreases with bed temperature.

Key words: Vortexing Fluidized Bed Combustor, Combustion Proportion, Biomass, Stability

INTRODUCTION

An improved fluidized bed combustion technique, known as the vortexing fluidized bed combustor (VFBC), has been developed for use as a small- or medium-scale boiler or incinerator. The concept of VFBC was originally presented by Sowards [1977]. It was consisted of a vortex-generating system which was formed by injecting secondary-air tangentially into the freeboard. To increase the residence time of unburned carbon in the freeboard and prevent the elutriation of fine particle from the fluidized bed, an integration of combustor and cyclone was developed by Korenberg [1983]. Based on Korenberg's concept, the vortexing fluidized bed combustor was developed and named by Nieh and Yang [1987]. The characteristics of the VFBC can be represented by the swirl flow within the freeboard.

Numerous experimental and theoretical works have been carried out to investigate the coal combustion mechanism in fluidized combustors in developing an efficient model for large scale fluidized bed combustors. Most of the published data concentrated on the carbon combustion mechanism. To simplify this problem, char or coal particles with low ash content were used in those studies to represent carbon particles. The volatile matter is assumed to be burned quickly [Atimtay, 1987]. Since the volatile matter is responsible for about 40% of the heat released in the combustor, it is imperative to know how fast volatile matter is released from the feedstock.

Biomass feedstock contains high volatile material content, 70-90% for woods vs. 30-45% for typical coals [Schiefelbein, 1989]. The potential contribution of biomass to the world's energy needs is greater than that of any other renewable energy. The gasification conversion process can be expected to supply a substantial portion of this contribution. However, the source and transportation costs for biomass materials restrict the amount of biomass that can be delivered to a central facility. In Taiwan, most farms are small and separated; therefore, instead of gasification, combustion may be a promising technology for biomass treatment. Previous research concentrated primarily on biomass gasification [Mariani et al., 1992; Miles and Miles, Jr., 1989].

Fluidized bed combustors have excellent heat and mass transfer characteristics, which have led to fluidization use in many large scale processes, such as fluidized catalytic cracking and fluidized coal combustion. Understanding and predicting the behavior of the fluidized bed process is often limited by our understanding of the underlying fluid-solid mixture mechanism. Instability manifests in gas fluidized beds as "bubbles." Bubbles are caused by the dynamics of particle movement. Bubbles reduce the contact efficiency between the fluid and particles and the heat and mass transfer. A two-fluid model linear equation has been used to investigate the stability of uniform fluidization [Pigford and Baron, 1965; Anderson and Jackson, 1968]. A nonlinear model has also been employed for analysis [Needham and Merkin, 1983; Ganser and Drew, 1990]. Most of these works were conducted from the micro-mechanism viewpoint.

The aim of this study is to understand the characteristics of a pilot scale VFBC for biomass combustion. In this study, the combustion efficiency, combustion proportion and bed stability are investigated under various operating conditions.

THEORY

1. Combustion Proportion

Fixed carbon was assumed burning in the bubbling bed. To know how the heat transfer surface should be arranged within the combustor to maintain a homogeneous temperature distribution, it is necessary to understand the heat proportion released in various sections in the combustor.

To simplify the mathematical calculation procedure, the following assumptions are made:

(1) The combustor is divided into three sections: bubbling bed,

†To whom correspondence should be addressed.
E-mail: cschyang@cycu.edu.tw

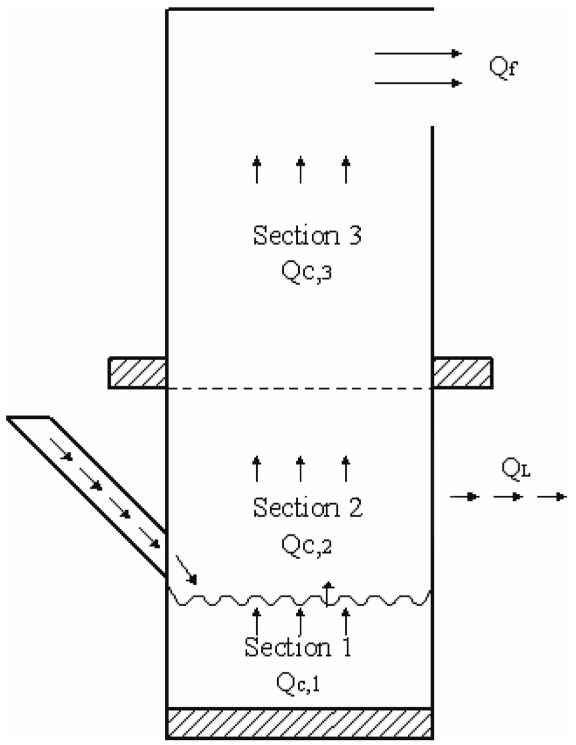

Fig. 1. Schematic diagram of three sections in combustor.

splash zone and freeboard (as showing in Fig. 1). Each section is assumed a continuous stirred tank reactor (CSTR).

(2) The specific heat of the flue gas (not including the water component) is similar to air.

(3) A drying process takes place in the bed.

(4) All of the water injected into the combustor is vaporized near the water injection location.

The mass balance of each section is shown as:

$$F_{in,i-1}+F_{air,i}+F_{feed,i}+F_{H_2O,i}-F_{out,i}=0 \quad (1)$$

The energy balance of each section is shown as:

$$Q_{c,i}+Q_{in,i}-Q_{out,i}-Q_{L,i}=0 \quad (2)$$

Where

$$Q_{in,i}=F_{air,i}(1-C)\int_{T_{ref}}^{T_{air}}Cp_{air}dT+F_{air,i}C\int_{T_{ref}}^{T_{air}}Cp_{H_2O(g)}dT +F_{H_2O,i}[\int_{T_{ref}}^{T_{H_2O}}Cp_{H_2O(l)}dT]+Q_{out,i-1} \quad (3)$$

$$Q_{out,i}=[F_{air,i}(1-C)+F_f(1-X_{H_2O}-9X_H\times y_i)] \times\int_{T_{ref}}^{T_i}Cp_{air}dT+[F_{air,i}C+F_f(X_{H_2O}+9X_H\times y_i)] \times\int_{T_{ref}}^{T_i}Cp_{H_2O(g)}dT+F_{H_2O,i}\times(\int_{T_{ref}}^{T_i}Cp_{H_2O(g)}dT+\lambda) \quad (4)$$

$$Q_{L,i}=\frac{(T_i-T_{sir,i})}{\frac{(r_b-r_a)}{2\pi r_1k_s}+\frac{(r_c-r_b)}{2\pi r_2k_c}}H_i \quad (5)$$

$$r_1=\frac{(r_b-r_a)}{\ln\left(\frac{r_b}{r_a}\right)} \quad (6)$$

$$r_2=\frac{(r_c-r_b)}{\ln\left(\frac{r_c}{r_b}\right)} \quad (7)$$

Where y_i is the extent of volatiles combustion in the i_{th} section, and y_i is calculated using the iteration method based on the mass and energy balances.

The combustion proportion in each section is given by Eq. (8).

$$X_{c,i}=\frac{Q_{c,i}}{\sum_{i=1}^{3}Q_{c,i}}\times 100\% \quad (8)$$

The temperatures in each section and combustor surface are measured. Integrating the mass and energy balance and heat loss calculations from the combustor surface, the combustion proportion (heat released) of each section can be calculated.

2. Stability Constant

To describe the stability of a bubbling fluidized bed combustor, the stability constant (τ) is proposed based on the following assumptions:

(1) The FBC bubbling bed is assumed to be a CSTR.

(2) The heat loss in the bubbling bed from the outside FBC surface can be neglected.

(3) The specific heats, Cp_s and Cp_{sand}, are assumed to be constant.

While step changing water injection is employed, the unsteady state energy balance can be expressed as:

$$W_bCp_{sand}\frac{dT_b}{dt}=Q_{gen,b}-F_{out}\int_{298}^{T_b}Cp_sdT \quad (9)$$

Where the F_{out} is the flow rate of the flue gas left from the bed surface and Cp_s is the specific heat of flue gas.

For mathematical algorithm convenience, the heat generated in the bubbling region, $Q_{gen,b}$, is expressed by the final temperature ($T_{b,\infty}$) at the steady state. Therefore, Eq. (9) can be transformed into the following:

$$W_bCp_{sand}\frac{dT_b}{dt}=F_{out}\int_{298}^{T_{b,\infty}}Cp_sdT-F_{out}\int_{298}^{T_b}Cp_sdT \quad (10)$$

When the variation in bed temperature is small, Cp_s can be assumed constant.

$$W_bCp_{sand}\frac{dT_b}{dt}=F_{out}Cp_s[(T_{b,\infty}-298)-(T_b-298)] \quad (11)$$

$$\frac{dT_b}{dt}=-\frac{F_{out}Cp_s}{W_bCp_{sand}}(T_b-T_{b,\infty})=-\frac{1}{\tau}(T_b-T_{b,\infty}) \quad (12)$$

The τ can be obtained by solving Eq. (12) with the initial conditions as follows:

I.C. $t=0, \quad T_b=T_{b,0}$ (13)

The stability constant can then be calculated by using Eq. (14).

$$\tau=-\frac{t}{\ln\left(\frac{T_b-T_{b,\infty}}{T_{b,0}-T_{b,\infty}}\right)} \quad (14)$$

3. Combustion Efficiency

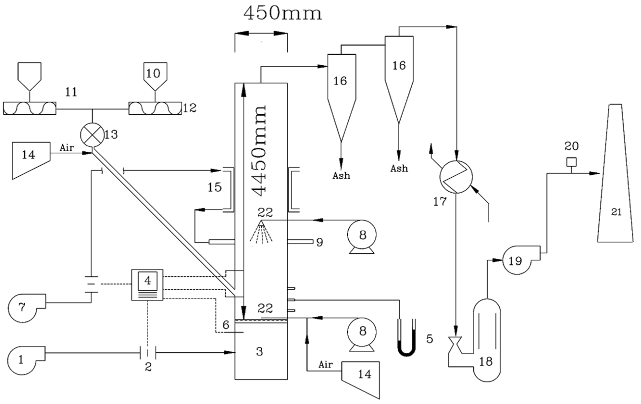

Fig. 2. Process flow chart of vortexing fluidized bed combustor.

1. Roots blower	12. Screw feeder
2. Orifice meter	13. Air lock
3. Windbox	14. Compressor
4. Recorder	15. Secondary air preheater
5. Manometer	16. Cyclone
6. Thermocouple	17. Shell and tube heat exchanger
7. Turbo blower	18. Scrubber
8. Water pump	19. Induced fan
9. Secondary air	20. Flue gas analyzer
10. Hopper	21. Stack
11. Vibrating feeder	22. Injection of cooling water

For different combustion systems, different formulas have been developed to calculate the combustion efficiency. In this work, the combustion efficiency is defined as the ratio of actual heat released in the combustor to the theoretical energy availability of a given feedstock and feed rate during the combustion process, i.e., Eq. (15).

$$\eta=\frac{Q_c}{F_f LHV_{feed}}\times 100\% \tag{15}$$

Where Q_c is the heat released in the combustor.

4. Experimental Approach

A schematic diagram of the combustion system is shown in Fig. 2. The fluidizing air (primary combustion air) was supplied by a 15 hp Roots blower and the secondary air was supplied by a 7.5 hp turbo blower. The combustor was 0.45m in diameter and 4.45 m in height. It was fabricated of stainless steel 316 and insulated with 150 mm thick Kaowool ceramic fiber. The feed material was supplied with the screw feeders. The feeding rate was controlled by adjusting the rotation speed of the drive motors. The feeding material went into the combustor through a chute located about 0.45 m above the air distributor. The system temperature was controlled by using in-bed and freeboard water injection.

The flue gas went through the air pollution control devices (APCD) and was cooled to about 200 °C before discharge into the atmosphere. The particulates in the flue gas were trapped by using two cyclones and a wet scrubber.

For a given operating condition, the temperature of the combustor was controlled by the in-bed injection water flow rate. Steady state was achieved when the temperature profiles were constant. Once the steady state condition was reached, the fly ash from the cyclones was weighed and collected for analysis. The operating conditions are summarized in Table 1.

Table 1. The experimental conditions

Primary air (Nm^3/min)	1.6-3.2
Secondary air (Nm^3/min)	0.2-1.8
Excess air (%)	20-100
Bed temperature (°C)	700-900
Freeboard temperature (°C)	850-950
Mean size of bed material (mm)	0.476
Bed weight (kg)	40-80

Table 2. The properties of feedstock

Proximate analyses	Rice husk	Corn	Soybean
Moisture	11.00	13.90	12.50
Volatile	60.25	69.20	74.13
Fixed carbon	14.87	15.54	8.24
Ash	13.88	1.36	5.13
Sum	100.00	100.00	100.00
LHV (WB) (kcal/kg)	2883	3261	4129
Apparent density (g/cm^3)	0.73	1.35	1.21

The feedstock used in this study were rice husks, corn and soybean biomass. Silica sand was used as the fluidized material. The approximate and ultimate analyses and physic properties of the feedstock are listed in Table 2.

RESULTS AND DISCUSSION

1. Temperature Distribution

The temperature distribution profiles within the combustor at various excess air ratios are shown in Fig. 3. Two peaks are observed on the temperature profile. The first is at 0.8 m above the gas distributor. This peak can be attributed to the large amount of volatile material ignited in this section. The second peak is just above the

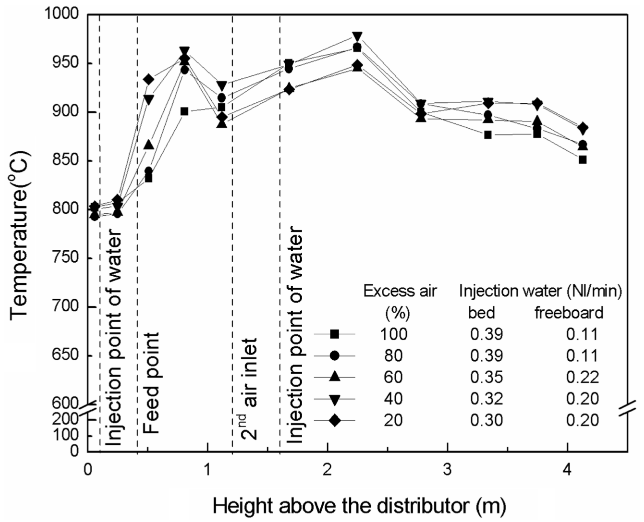

Fig. 3. Temperature distribution in the VFBC with various primary air flow rates (corn=15.9 kg/hr, soybean=18.6 kg/hr, static bed height=0.24 m, secondary air flow rate=0.6 Nm^3/min, feeding purge air=0.2 Nm^3/min).

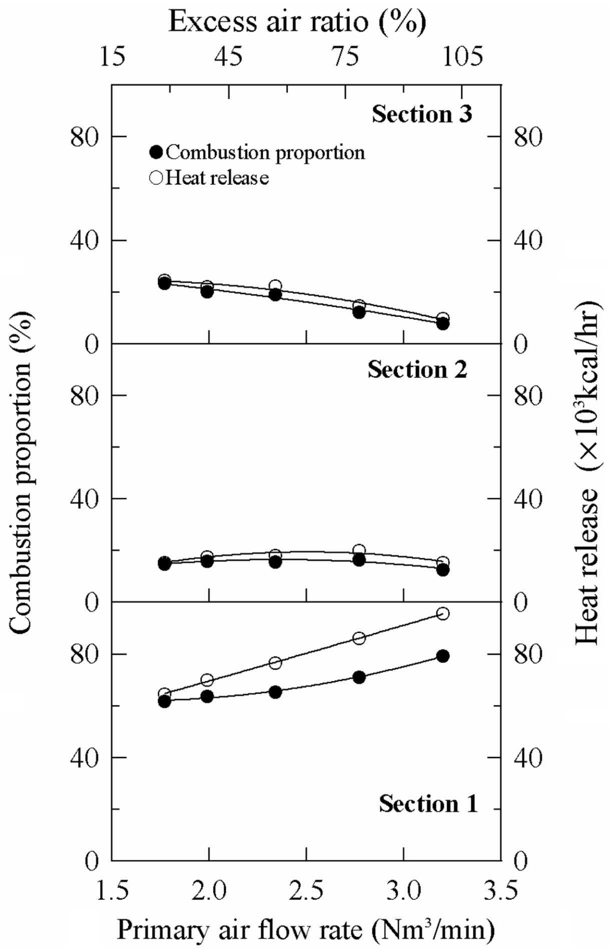

Fig. 4. Effect of primary air flow rate on combustion proportion (corn=15.9 kg/hr, soybean=18.6 kg/hr, static bed height=0.24 m, secondary air flow rate=0.6 Nm^3/min, feeding purge air=0.2 Nm^3/min, temperature=800 °C).

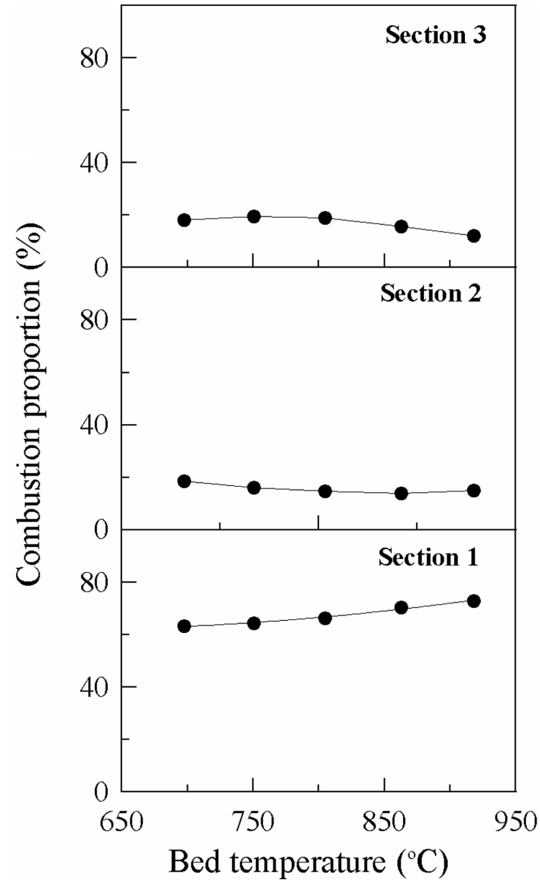

Fig. 5. Effect of bed temperature on combustion proportion (corn=15.9 kg/hr, soybean=18.6 kg/hr, static bed height=0.24 m, primary air flow rate=2 Nm^3/min, secondary air flow rate=0.6 Nm^3/min, feeding purge air=0.2 Nm^3/min).

secondary air injection location. This peak is caused by the combustion of unburned carbon and volatiles resulting from the fresh injected air. The results, shown in Fig. 3, demonstrate that to maintain the bed temperature at 800 °C, the amount of water injected with primary air must be increased. This is attributed to the in-bed combustion proportion increasing with the excess primary air ratio.

Because the volatile and ignited carbons are nearly exhausted at the exit and the heat was lost from the combustor surface, the temperature detected at the freeboard exit is lowest.

2. Combustion Proportion

Fig. 4 shows the primary air flow rate effect on the combustion proportion. The results shown in Fig. 4 reveal that the in-bed combustion proportion increases significantly with the increase in primary air flow rate. This is attributed to the increase in excess air and combustible mixing with the air as the primary air flow rate increases. Both factors, excess air and mixing, can enhance the reaction rate of combustibles with air in the bed. The results obtained in this study are in agreement with that obtained by Bautista-Margulis et al. [1996].

Fig. 5 shows the bed temperature effect on the combustion proportion in each section. The combustion proportion in the bubbling region increases with the bed temperature. This is attributed to the higher reaction rate at higher bed temperature.

Corn and soybeans exhibit different volatile/fixed-carbon ratios. The volatile/fixed-carbon ratio can be adjusted by changing the corn and soybean feed rates. The results, as shown in Fig. 6, demonstrate that the combustion proportion in the bubbling region decreases with the volatile/fixed-carbon ratio. This is in agreement with the statement that most of the fixed carbon is burned in the bubbling bed and most volatiles are burned in the freeboard.

For the same test, the volatile/fixed-carbon ratio was adjusted by changing the rice husk and soybean feed rates, respectively. The combustion proportion in the bubbling region increases with increasing volatile/fixed-carbon ratio, as shown in Fig. 7, which is contrary to the result shown in Fig. 6. This is attributed to the higher elutriation rate of rice husks because of its lower density. Rice husks rose with the gas flow and burned in the freeboard. As shown in Figs. 6 and 7, the results demonstrate that the feedstock characteristics significantly affect the combustion proportion in each section.

3. Combustion Efficiency

Combustion behavior is represented by the combustion efficiency. Therefore, the effects of various operating parameters on the combustion efficiency are investigated in this section. Fig. 8 shows the primary air flow rate effect on the combustion efficiency when the secondary air flow rate is kept constant. From Fig. 8, the combustion efficiency increases with the increase in primary air flow rate.

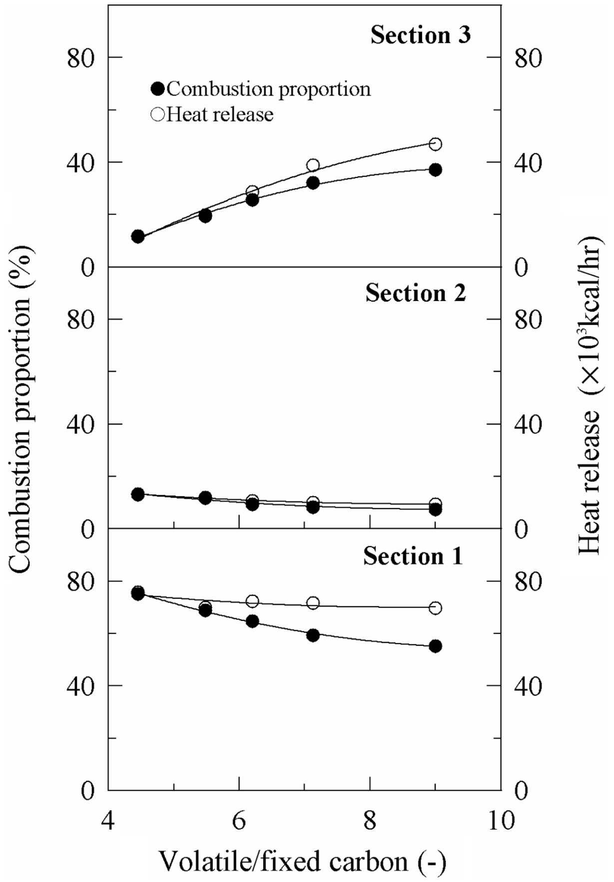

Fig. 6. Effect of volatile/fixed carbon ratio on combustion proportion (corn=0-35.1 kg/hr, soybean=0-33.1 kg/hr, static bed height=0.24 m, bed temperature=800 °C, excess air ratio=40%, in-bed stoichiometric air ratio=100%, feeding purge air=0.2 Nm^3/min).

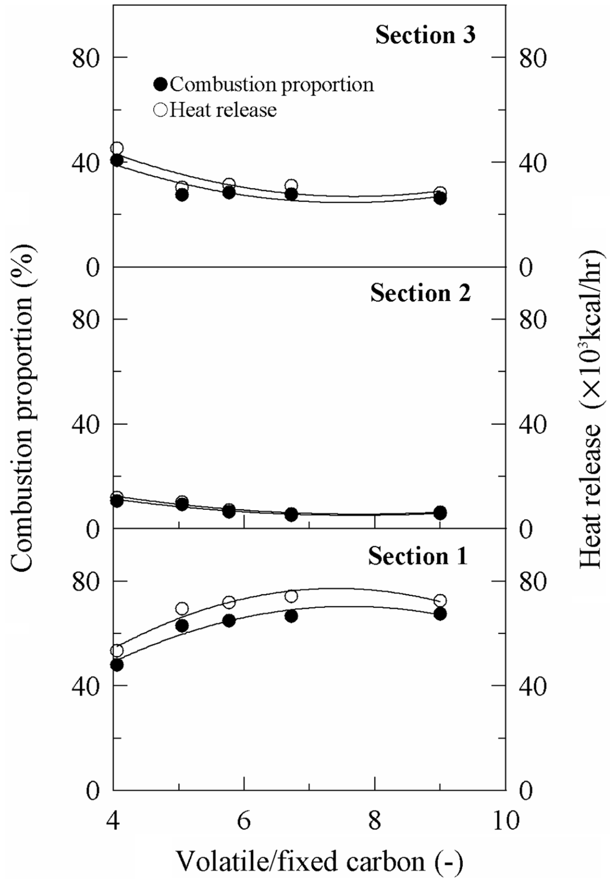

Fig. 7. Effect of volatile/fixed carbon ratio on combustion proportion (rice husk=0-41.6 kg/hr, soybean=0-33.1 kg/hr, static bed height=0.24 m, bed temperature=800 °C, excess air ratio=40%, in-bed stoichiometric air ratio=100%, feeding purge air=0.2 Nm^3/min).

This is attributed to higher turbulence and in-bed excess air ratio caused by increasing the primary air flow rate. Higher turbulence and in-bed excess air lead to better gas-solid contact and higher oxygen mass transfer rate to the fuel particle surface. Therefore, the char combustion rate in the bubbling bed increases as the superficial velocity increases [Winter et al., 1997]. These results also imply that the oxygen concentration and gas-solid mixing in the bed are the dominant factors for combustion.

The effect of in-bed stoichiometric air percent ratio on the combustion efficiency at a given excess air ratio of 40% was studied (Fig. 9). From Fig. 9, the deviation between the maximum and minimum combustion efficiency values is within 3%. Therefore, we can state that the in-bed stoichiometric air percent ratio (or primary to secondary air ratio) effect can be neglected. The bed height effect (or bed weight) on the combustion efficiency, as shown in Fig. 10, is also minimal. In these two experiments, the superficial gas velocities and combustion temperatures were kept the same; therefore, the combustible residence times in the combustor were similar. Two most important factors in combustion efficiency (combustion temperature and residence time) were not changed with the varying of experimental variables. Consequently, the combustion efficiencies are not changed with the in-bed stoichiometric air percent ratio and bed height.

To understand the volatile/fixed-carbon ratio effect on the combustion efficiency, corn and soybean mixtures were used as the feedstock. The volatile/fixed-carbon ratios were adjusted by changing the corn feed rate range from 0 to 35.1 kg/hr and the soybean range from 0 to 33.1 kg/hr. According to the results shown in Fig. 11, the combustion efficiency increased with the increase in volatile/fixed-carbon ratio. This is caused by the amount of unburned char particles. In this study, the heat losses are considered two possibilities, the apparatus heat loss from the surface of combustor and the unburned char particle elutriated. The higher the volatile/fixed carbon ratio leads the less unburned char particles discharge. Consequently, the low probability for char particles elutriation and high volatile combustion rate, the overall combustion efficiency will increase with the volatile/fixed-carbon ratio. This statement is in agreement with the results of Paul et al. [1993], obtained from a fluidized bed combustor using coal of various rank as the feedstock. They found that the higher the fixed carbon content, the lower the combustion efficiency.

4. Bed Stability

One of the most important advantages of the fluidized bed combustor (FBC) is the bed temperature inertia. The bubbling bed serves as a heat reservoir, maintaining bed temperature while the feedstock heating value is always changing. The stability constant, τ, is used

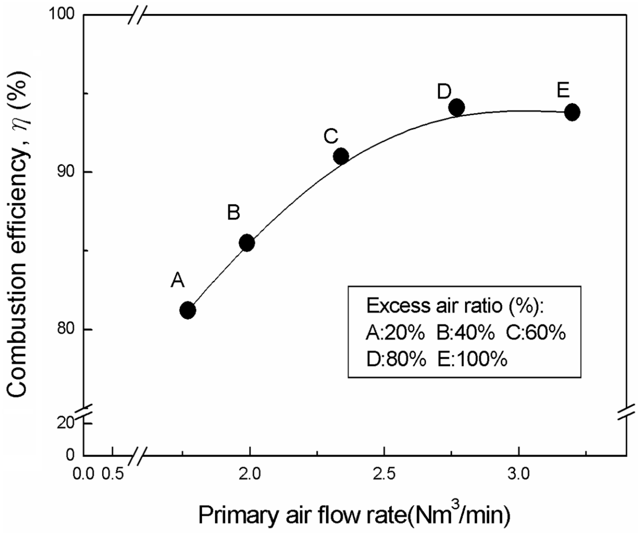

Fig. 8. Effect of primary air flow rate on combustion efficiency (corn=15.9 kg/hr, soybean=18.6 kg/hr, static bed height=0.24 m, secondary air flow rate=0.6 Nm^3/min, feeding purge air =0.2 Nm^3/min, temperature=800 °C).

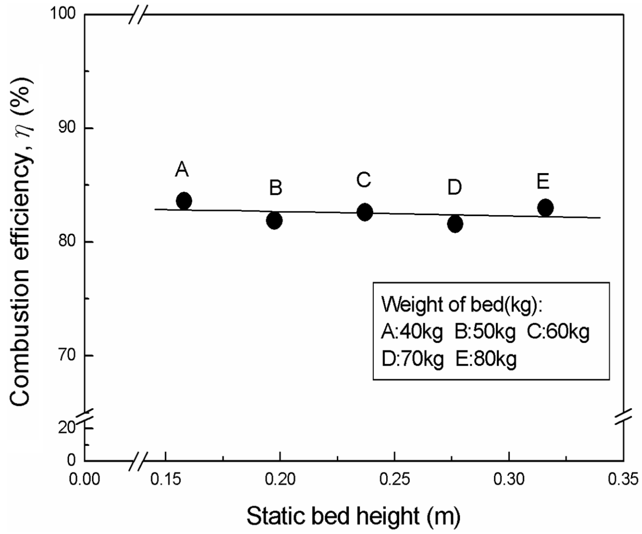

Fig. 10. Effect of static bed height on combustion efficiency (corn= 15.9 kg/hr, soybean=18.6 kg/hr, bed temperature=800 °C, primary air flow rate=2.0 Nm^3/min, excess air ratio=40%, in-bed stoichiometric air percent ratio=100%, feeding purge air=0.2 Nm^3/min).

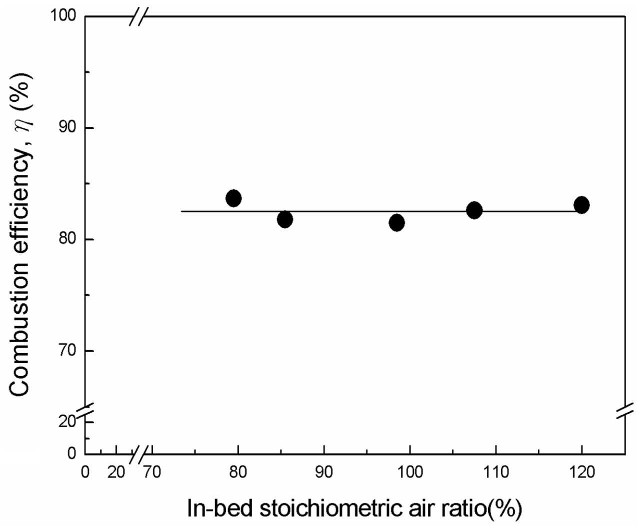

Fig. 9. Effect of in-bed stoichiometric air percent ratio on combustion efficiency (static bed height=0.24 m, primary air flow rate=2.0 Nm^3/min, excess air ratio=40%, feeding purge air= 0.2 Nm^3/min, temperature=800 °C).

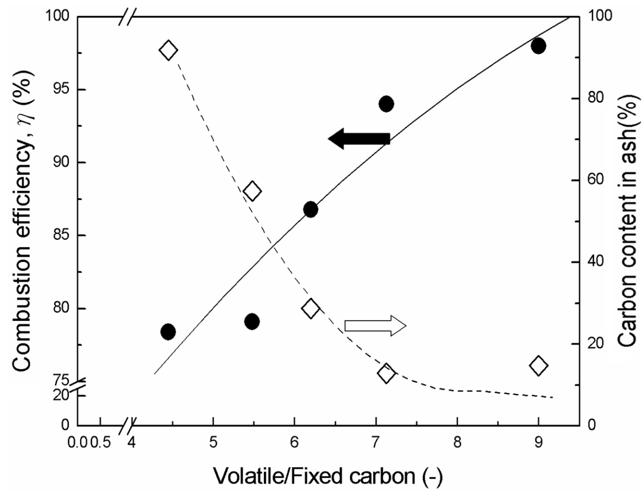

Fig. 11. Effect of volatile/fixed carbon on combustion efficiency (corn=35.1-0 kg/hr, soybean=0-33.1 kg/hr, static bed height =0.24 m, bed temperature=800 °C, excess air ratio=40%, in-bed stoichiometric air ratio=100%, feeding purge air =0.2 Nm^3/min).

to represent the stability of the fluidized bed. A higher stability constant implies that the system is more stable.

The stability constant, τ, was calculated from the bed temperature history variation data produced by the step change in cooling water injected into the bed. The step change of cooling water injection worked as a disturbance of feedstock heating value. When a certain set combustion condition was achieved, the rate of cooling water injection would be changed suddenly and sustained this new change. The dynamic behaviors of bed temperature change were collected and analyzed via Eq. (14). The bed weight, primary air rate and initial bed temperature effects on the stability were investigated.

All of the experiments conducted for the stability test were preceded using a fuel-feeding rate of 15.9 kg/hr for corn and 18.6 kg/hr for soybeans. Most of the experiments were conducted at a 40% excess air ratio (variables of bed weight and bed temperature). When a step change in water injection (0.1 L/min) was employed, the bed temperature vs. time data were recorded and analyzed. A typical result is shown in Fig. 12. The stability constant, τ, is in agreement with a first order equation, as shown in Eq. (14).

As shown in Fig. 13, the stability constant, τ, increases with the bed weight. This is attributed to heat sink effect in the bed. The bed heat capacity increases when the bed weight increases. In other words, the higher the bed weight, the less sensitive the bed is to tempera-

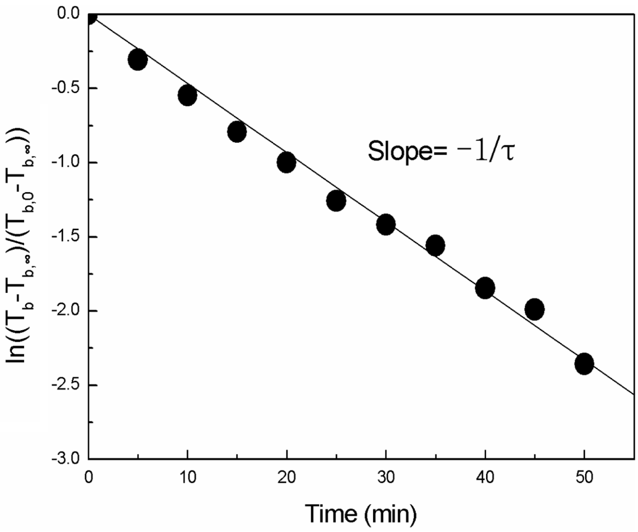

Fig. 12. Typical temperature changes in bed after increasing water injected by step change (corn=15.9 kg/hr, soybean=18.6 kg/hr, excess air ratio=40%, in-bed stoichiometric air ratio=100%, feeding purge air=0.2 Nm³/min).

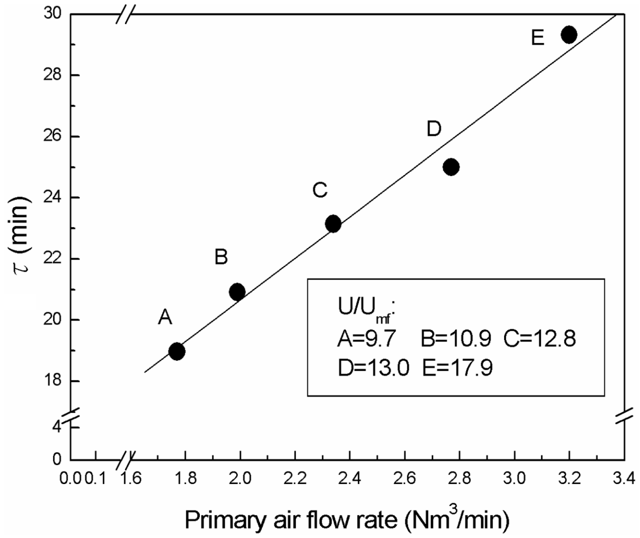

Fig. 14. Effect of primary air flow rate on stability constant (corn=15.9 kg/hr, soybean=18.6 kg/hr, static bed height=0.24 m, secondary air flow rate=0.6 Nm³/min, feeding purge air =0.2 Nm³/min, temperature=800 °C).

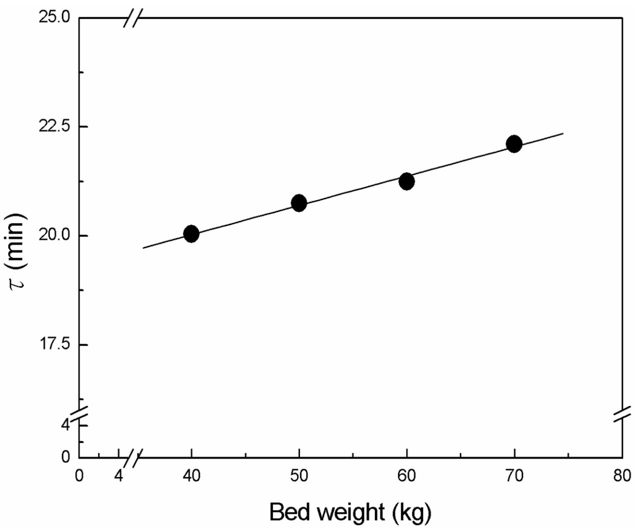

Fig. 13. Effect of bed weight on stability constant (corn=15.9 kg/hr, soybean=18.6 kg/hr, excess air ratio=40%, in-bed stoichiometric air ratio=100%, feeding purge air=0.2 Nm³/min, temperature=800 °C, U/U_{mf}=10.9).

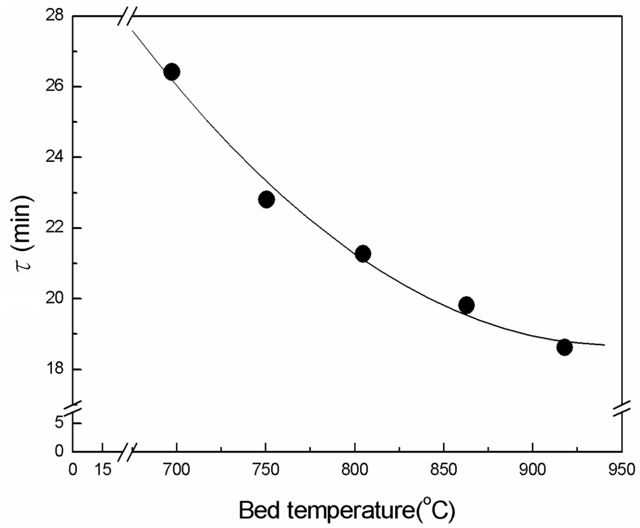

Fig. 15. Effect of bed temperature on stability constant (corn=15.9 kg/hr, soybean=18.6 kg/hr, static bed height=0.24 m, secondary air flow rate=0.4 Nm³/min, in-bed stoichiometric air ratio=100%, feeding purge air=0.2 Nm³/min, U/U_{mf}=10.9).

ture (feedstock heating value) changes.

From Fig. 14, one can find that at a certain temperature the stability constant increases with the flow rate of primary air. And from Fig. 15 the results illustrate that the stability constant decreases with bed temperature. The stability constant is indicative of the speed of response of the process and depends on the operating conditions. In this study, we have only limited information on the effects of primary air flow rate and bed temperature. The simple tests of this study are not enough to interpret completely and accurately. Therefore, further studies are needed to clarify these phenomena. Even though the mechanisms of the bed temperature stability are not clear, an empirical correlation is developed to predict the bed temperature stability constant. Using regression analysis, a relation

$$\tau = 4.588\times10^{-4}\times\frac{(W_b+258.51)(Q_1+1.2105\times10^{-3}(T_b+273.15))}{(T_b+273.15)^{5/3}} \quad (16)$$

was obtained that correlates all of the experimental data obtained in this study with an average deviation of 2.1%, and standard deviation of 3.0%, as shown in Fig. 16. The agreement between the estimated values and the experimental data is good.

CONCLUSION

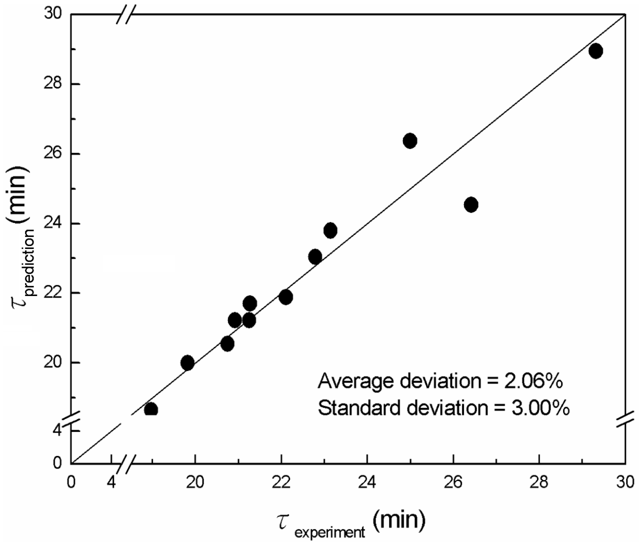

Fig. 16. Comparison between experimental and predicted stability constant.

In this study, the bed temperature within a combustor was controlled by using water injected into a fluidized bed combustor. The bed excess air ratio was the major parameter for combustion efficiency. The combustion efficiency increased with the increase in primary air flow rate (excess air ratio) bed temperature and feedstock volatile/fixed carbon ratio. The bed height effect on the combustion efficiency was minimal.

A higher combustion proportion within a bubbling bed can be obtained by increasing the bed temperature or primary air flow rate. The combustion proportion within the bed decreased with the volatile/fixed carbon ratio when the feedstock was mixture of soybeans and corn. This is in agreement with our inference. However, the combustion proportion within the bed increased with the increase in volatile/fixed carbon ratio when the feedstock was a mixture of rice husks and soybeans. Rice husk elutriation into the freeboard was the dominant factor for heat released in the freeboard.

The inertia of a fluidized bed combustor can be represented by the stability constant, which increases with the bed weight, primary air flow rate, and decreases with the bed temperature. An empirical correlation was proposed to express the relationship between the stability constant and operating conditions such as bed weight, bed temperature and primary air flow rate. The agreement between the estimated values and experimental data is good.

NOMENCLATURE

C : moisture of air [kg/kg]
Cp_{air} : specific heat capacity of air [kcal/kg-°C]
$Cp_{H_2O(l)}$: specific heat capacity of liquid water [kcal/kg-°C]
$Cp_{H_2O(g)}$: specific heat capacity of gaseous water [kcal/kg-°C]
Cp_s : specific heat capacity of flue gas [kcal/kg-°C]
Cp_{sand} : specific heat capacity of sand [kcal/kg-°C]
F_{air} : air mass flow rate [kg/min]
F_f : feeding rate [kg/min]
F_{H_2O} : injection water flow rate [kg/min]
F_{in} : input gas mass flow rate [kg/min]
F_{out} : output gas mass flow rate [kg/min]
H_i : height of the ith section [m]
k_s : thermal conductivity of s.s. 316 [kcal/m-min-°C]
k_c : thermal conductivity of ceramic fiber [kcal/m-min-°C]
LHV_{feed} : wet base low heating value of feedstock [kcal/kg]
Q_1 : flow rate of primary air [Nm^3/min]
Q_c : total heat release in combustor [kcal/min]
$Q_{c,i}$: heat release of ith section [kcal/min]
Q_f : heat loss with flue gas exhausting [kcal/min]
$Q_{gen,b}$: heat generation from fuel combustion in bed [kcal/min]
Q_{in} : input heat [kcal/min]
Q_L : heat loss from surface of combustor [kcal/min]
Q_{out} : output heat [kcal/min]
T_{air} : temperature of inlet air [°C]
T_b : bed temperature [°C]
$T_{b,0}$: initial bed temperature [°C]
$T_{b,\infty}$: final bed temperature [°C]
T_i : temperature of the ith section [°C]
T_{H_2O} : temperature of injected water [°C]
T_{ref} : reference temperature, 25 °C [°C]
T_{sur} : temperature of combustor surface [°C]
r_1 : logarithmic mean radius [m]
r_2 : logarithmic mean radius [m]
r_a : inner diameter of combustor [m]
r_b : outer diameter of combustor [m]
r_c : outer diameter of combustor with insulation [m]
W_b : bed weight [kg]
$X_{c,i}$: combustion proportion of the ith section [-]
X_{H_2O} : weight percentage of water in feedstock [-]
X_H : weight percentage of H element in feedstock [-]
y_i : combustion extent of volatiles in the ith section [-]
η : combustion efficiency [-]
λ : latent heat of water [kcal/kg]
τ : stability constant [min]

REFERENCES

Anderson, T. B. and Jackson, R., "Fluid Mechanical Description of Fluidized Beds," *Ind. Eng. Chem. Fundam.*, **7**(1), 12 (1968).

Atimtay, A. T., "Combustion of Volatile Matters in Fluidized Bed," *Ind. Eng. Chem. Res.*, **26**, 452 (1987).

Bautista-Margulis, R. G., Siddall, R. G. and Manzanares-Papayanopouls, L. Y., "Combustion Modeling of Coal Volatiles in the Freeboard of a Calorimetric Fluidized Bed Combustor," *Fuel*, **75**(15), 1737 (1996).

Ganser, G. H. and Drew, D. A., "Nonlinear Stability Analysis of a Uniformly Fluidized Bed," *Int. J. Multiphase Flow*, **16**(3), 447 (1990).

Korenberg, J., "Integrated Fluidized Bed/Cyclone Combustion Development," *Proc. 4th. Int. Conf. on Fluidization*, Kunii, D. and Tori, R., eds., 491 (1983).

Mariani, G., Benefenati, E., Fanelli, R., Nicoli, A., Bonfitto, E. and Jacopone, S., "Incineration of Agroindustrial Waste and Macropollutants and Micropollutants Emission," *Chemosphere*, **24**(11), 1545 (1992).

Miles, T. R. and Miles, T. R., Jr., "Overview of Biomass Gasification in the USA," *Biomass*, **18**(3-4), 163 (1989).

Needham, D. J. and Merkin, J. H., "Propagation of a Voidage Distribution in a Uniformly Fluidized Bed," *J. Fluid Mech.*, **131**, 427 (1983).

Nieh, S. and Yang, G., "Particle Flow Pattern in the Freeboard of a Vortexing Fluidized Bed," *Powder Technol.*, **50**, 121 (1987).

Paul, J., Peeler, K. and Lane, G. L., "Relation Between Combustion Efficiency and Coal Rank in Fluidized Bed Combustor," *Fuel*, **72**, 73 (1993).

Pigford, R. L. and Baron, T., "Hydrodynamic Stability of Fluidized Bed," *Ind. Eng. Chem. Fundam.*, **4**, 81 (1965).

Schiefelbein, G. F., "Biomass Thermal Gasification Research: Recent Results from the Unite States DOE's Research Program," *Biomass*, **19**, 145 (1989).

Sowards, N. K., US Patent No. 4060041 (1977).

Winter, F., Prah, M. E. and Hofbauer, H., "Temperature in a Fuel Particle Burning in a Fluidized Bed: The Effect of Drying, Devolatilization, and Char Combustion," *Combustion and Flame*, **108**, 302 (1997).